Precise Epitope Mapping of Malaria Parasite Inhibitory Antibodies by TROSY NMR Cross-Saturation†

William D. Morgan,*,‡ Thomas A. Frenkiel,§ Matthew J. Lock,‡ Munira Grainger,‡ and Anthony A. Holder‡

Division of Parasitology and MRC Biomedical NMR Centre, National Institute for Medical Research, The Ridgeway, Mill Hill, London NW7 1AA, United Kingdom

Received August 9, 2004; Revised Manuscript Received October 11, 2004

ABSTRACT: We have applied NMR cross-saturation with TROSY detection to the problem of precisely mapping conformational epitopes on complete protein antigen molecules. We have investigated complexes of the Fab fragments of two antibodies that have parasite inhibitory activity, bound to the important malaria vaccine candidate antigen, *Plasmodium falciparum* $MSP1_{19}$. The results indicate remarkable overlap between these epitopes for inhibitory antibodies, and will provide a basis for theoretical modeling of the antibody−antigen interface.

The major merozoite surface protein-1 (MSP1)[1] of the malaria parasite *Plasmodium falciparum* is of considerable interest as a vaccine candidate antigen. Monoclonal antibodies that bind to the C-terminal fragment of MSP1 (designated $MSP1_{19}$, and consisting of an EGF module pair) have the ability to inhibit erythrocyte invasion and MSP1 proteolytic processing in vitro as well as invasion in rodent models. Antibodies that inhibit processing also inhibit invasion, suggesting that this is the mechanistic basis of their activity. However, parasite inhibitory activity is limited to a small subset of anti-$MSP1_{19}$ antibodies. It is therefore important to characterize the epitope and other binding characteristics of such parasite inhibitory antibodies. In particular, two monoclonal antibodies, 12.8 and 12.10, have been examined in several studies. Some knowledge of antigen recognition has been provided by methods such as peptide ELISA and amino acid replacements (*1*). Both electron microscopy and NMR chemical shift perturbation demonstrated that these two inhibitory antibodies were topographically distinct from the "neutral" or noninhibitory antibody 2F10 (*2*, *3*).

Rapid epitope mapping by chemical shift perturbation, using TROSY techniques (*4*, *5*), produced a reliable but necessarily approximate view of antibody−antigen interfaces (*3*). NMR cross-saturation has been demonstrated to provide a more precise view of protein−protein and protein−nucleic acid interfaces, through direct transfer of magnetization from one molecule to another, which occurs over a limited distance (*6*). Here we show for the first time the utility of TROSY cross-saturation experiments in mapping antibody−antigen contact surfaces, and apply this approach to determining more precisely the epitopes recognized by the two parasite inhibitory antibodies, 12.8 and 12.10. We have also assigned the shifted signals in the bound complexes using triple-resonance experiments, permitting quantitative determination of the degree of chemical shift perturbation.

MATERIALS AND METHODS

Expression, Isotope Labeling, and Purification of P. falciparum $MSP1_{19}$ and Antibodies. The ^2H-, ^{15}N-, and ^{13}C-labeled compound was expressed and purified from the methylotrophic yeast *Pichia pastoris* as described previously (*3*), except that the medium also contained ^{13}C source compounds in this case. All isotopes were obtained from Cambridge Isotope Laboratories. Initial cultures were grown in 99.8% D_2O minimal medium containing 0.5% [$^{13}C_6$]glucose as the carbon source. Expression was induced by transfer to a 0.5% methanol medium, with [^{13}C]methanol-d_4 as the carbon source. As a final step, the N-terminal His tag was removed by factor Xa digestion (New England Biolabs), and the products were separated by size exclusion chromatography with a Superdex 75 column. The resulting $MSP1_{19}$ protein contained a single His residue preceding Asn1 of the antigen.

$MSP1_{19}$ samples produced in D_2O media contain several protected amide backbone groups that do not exchange with solvent under normal conditions, and remain deuterated. These protected amides were exchanged for protons by heating the protein in NMR sample buffer (see below) at 65 °C for 1 h. At this temperature, the secondary structure is labile, but the protein is not denatured, as shown by HSQC spectra (data not shown). The 12.8 and 12.10 monoclonal antibodies and their Fab fragments were prepared as described previously (*3*).

The complexes were formed by titrating the labeled $MSP1_{19}$ antigen with unlabeled Fab fragments, and observing the disappearance of the free antigen cross-peaks from the $^1H-^{15}N$ correlation spectra. The final molar ratio of the Fab fragment to $MSP1_{19}$ was approximately 1.25:1.

† Research was supported by the Medical Research Council and by the European Commission through the EUROMALVAC Consortium, Contracts QLK2-CT-1999-01293 and QLK2-CT-2002-01197.

* To whom correspondence should be addressed: Division of Parasitology, National Institute for Medical Research, The Ridgeway, Mill Hill, London NW7 1AA, United Kingdom. Phone: +44 208 8162134. Fax: +44 208 8162370. E-mail: wmorgan@nimr.mrc.ac.uk.

‡ Division of Parasitology.

§ MRC Biomedical NMR Centre.

[1] Abbreviations: TROSY, transverse relaxation-optimized spectroscopy; MSP1, merozoite surface protein 1; $MSP1_{19}$, MSP1 C-terminal EGF module pair; HSQC, heteronuclear single-quantum correlation.

10.1021/bi0482957 CCC: $30.25
Published on Web 12/21/2004

NMR Spectroscopy. NMR spectra were acquired with a Varian INOVA spectrometer, operating at a magnetic field strength of 18.8 T, in a buffer containing 10 mM sodium phosphate and 50 mM NaCl (pH 6.5) in a 90% H_2O/10% D_2O mixture at 25 °C. The concentration of $MSP1_{19}$−Fab fragment complexes was 1 mM, in a volume of 0.33 mL. Spectra were processed and analyzed with NMRPipe/NMRDraw (*7*) and Sparky (T. D. Goddard and D. G. Kneller, University of California, San Francisco).

Cross-saturation experiments were carried out using a TROSY pulse sequence with water flip-back (*4*, *5*). The overall recording time for each experiment was approximately 2 h, with a t_{1max} of 20 ms. Cross-saturation was performed by irradiation with a band-selective inversion pulse centered at a frequency of 1.3 ppm with a bandwidth of 2.8 ppm. A set of spectra were acquired with saturation periods from 0.2 to 1.6 s. An interleaved control spectrum was acquired simultaneously with each cross-saturation spectrum, with the irradiation frequency displaced to −14 ppm, well outside the range of antibody proton resonances. Cross-peaks in two-dimensional spectra were quantified with the nLinS script of NMRPipe. The relative intensity of each cross-peak is the integrated peak volume of the cross-saturation spectrum divided by the corresponding value for the control spectrum.

Although some spin diffusion seemed to occur within the antigen molecule, this did not preclude mapping the residues that are most sensitive to cross-saturation. The spin diffusion must occur by NH−NH transfers, as the antigen protein is highly deuterated at carbon-bonded positions (∼99% as determined by mass spectrometry). It would be expected to occur to a greater extent in regions with α-helical secondary structure, where there is a network of relatively short NH−NH distances, but this type of secondary structure does not occur in $MSP1_{19}$. If necessary, the number of these NH−NH transfers could be reduced by using samples that have been prepared in solvent mixtures containing a higher proportion of D_2O than the 10% used here such that solvent exchange gives a higher level of fractional deuteration of the backbone amide groups (*6*). This would enable a more precise contact distance determination, but at the cost of reduced sensitivity, and was not thought to be justified in this case.

The two Fab fragments bind tightly to the $MSP1_{19}$ antigen, and NMR data indicated that the complexes were in slow exchange on the NMR time scale (*3*). This was confirmed by surface plasmon resonance experiments, which showed that the dissociation rate constants for these Fab complexes were in the range of 10^{-5}−10^{-6} s^{-1} (M. J. Lock, unpublished data). This precludes any significant chemical exchange effects on the time scale of the cross-saturation experiments.

Three-dimensional HNCO, HNCA, and HNCACB TROSY triple-resonance assignment experiments were carried out using the pulse sequences of Yang and Kay (*8*). The HNCACB experiment was optimized for detection of the C_β signals. The total experiment time was 16 h for HNCO, 1 day for HNCA, and 4 days for HNCACB experiments. The values of t_{1max} for the ^{15}N dimension were ca. 12 ms for the HNCO experiments and in the range of 15−19 ms for the HNCA and HNCACB experiments. The maximum acquisition times in the carbon dimensions were 14 ms for the HNCO experiments and ca. 6.5 ms for the HNCA and HNCACB experiments.

More than 80% of the non-proline residues in each bound complex could be assigned. Cross-peaks for a few residues appeared to be weak or absent, perhaps due to intermediate exchange between multiple conformations, or enhanced solvent exchange. These residues, near the N- and C-termini, could not be assigned in the triple-resonance spectra or monitored for cross-saturation, and might form additional antibody contacts that have not been identified.

Normalized weighted average chemical shift perturbation values were calculated with the formula (*6*)

$$\Delta\ (\mathrm{ppm}) = [(\Delta^1\mathrm{H})^2 + (0.15\Delta^{15}\mathrm{N})^2]^{1/2}$$

Structures were imaged and analyzed with Insight2 (Accelrys).

RESULTS

TROSY experiments with cross-saturation were performed with complexes of either Fab 12.8 or Fab 12.10, and perdeuterated ^{13}C- and ^{15}N-labeled *P. falciparum* $MSP1_{19}$ antigen. Residues at the contact interface were identified by monitoring attenuation of the $MSP1_{19}$ $\{^1H-^{15}N\}$ TROSY cross-peaks, after saturating irradiation of aliphatic methyl region protons in the non-isotope-labeled Fab fragment. The residues that were most sensitive to cross-saturation in the bound complexes were also significantly shifted from their normal frequencies in the free antigen spectrum. Therefore, it was necessary to perform a set of triple-resonance backbone assignment experiments to identify these signals (*8*). Resonance assignment lists for the free ^2H-, ^{15}N-, and ^{13}C-labeled $MSP1_{19}$ protein, as well as the bound $MSP1_{19}$ antigen in the Fab 12.8 and Fab 12.10 complexes, are given in Table 1 of the Supporting Information.

Spectra of the Fab 12.8− and Fab 12.10−$MSP1_{19}$ complexes are shown in Figures 1 and 2. The most sensitive residues were reduced to a value of <50% of that of the nonirradiated control sample at the maximum saturation time point (five residues in the Fab 12.8 complex, Gln14−Cys18, and six residues in the Fab 12.10 complex, Gln6, Cys7, and Asn15−Cys18).

The complete time series is shown in Figure 1 of the Supporting Information for two sample cross-peaks, Ser16 and Gly68. Neither residue was attenuated significantly by cross-saturation with the free $MSP1_{19}$ antigen. This was also the case for all cross-peaks in the free antigen spectra. Gly68 is scarcely affected in either antibody complex, whereas Ser16 in the Fab 12.8 complex exhibited the highest sensitivity of any residue, reaching a final value of 20% of the initial intensity. The residues that display these high levels of sensitivity have backbone amide groups located near antibody protons in the bound complexes [within ∼7 Å, as estimated by Takahashi and co-workers (*6*)]. The full time course of cross-saturation experiments for all of the most sensitive residues in each Fab complex is shown in Figure 2 of the Supporting Information. The kinetics are broadly similar for all of these residues. Residues 15 and 16 in the Fab 12.8 complex show the greatest response and may thus represent an especially close antibody contact with the $MSP1_{19}$ backbone here.

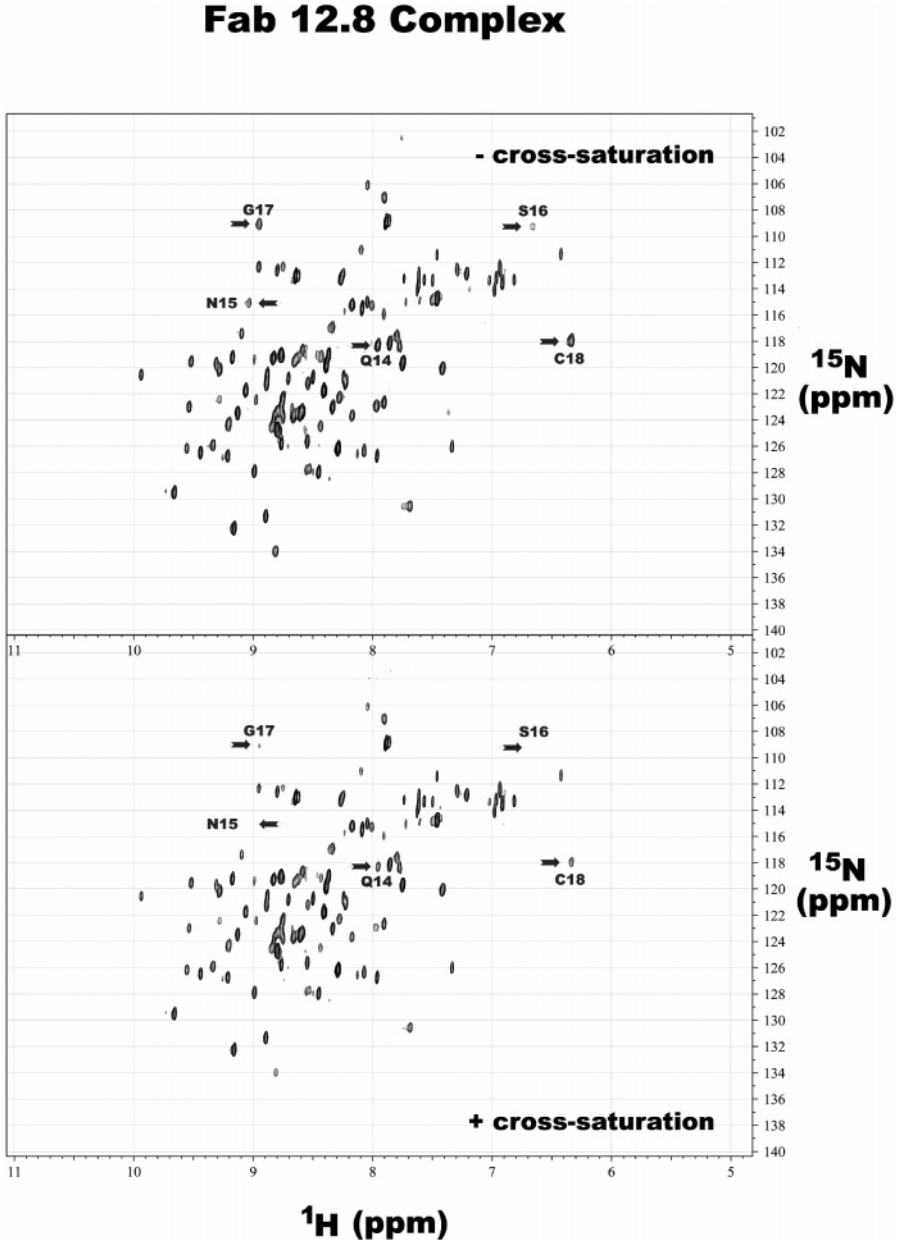

FIGURE 1: TROSY spectra of the Fab 12.8 complex with (bottom panel) and without (top panel) cross-saturation, with a saturation time of 1.6 s. The most sensitive residues (less than 50% relative intensity) are denoted with arrows.

With each Fab fragment, the most sensitive residues (Figure 3A,B) are tightly clustered in a single region of the three-dimensional structure of the antigen (Figure 4). It is particularly striking that there is also a very high degree of overlap between the most affected residues for the two antibodies, with four of these residues being identical in both complexes. Intermediate effects (a final level of 50−60% intensity) occurred at residues Phe19, Glu27, Phe87, and Asp88 in the Fab 12.8 complex and at residues His5, Phe19, Arg20, Leu31, and Gly89 in the Fab 12.10 complex. This may reflect either a longer distance from the antibody protons or possibly a secondary transfer of saturation via the more sensitive contact residues.

The residues that were subjected to large chemical shift perturbation in the bound complexes are shown in panels C and D of Figure 3 and Figure 4. A total of 12 were identified in the 12.8 complex and 15 residues in the 12.10 complex. There is a high level of agreement with the cross-saturation results: 10 of the 11 residues most sensitive to cross-saturation also exhibited significant shift perturbation. However, it is interesting to note that some residues displayed large chemical shift perturbations, but not high cross-saturation sensitivity. For the Fab 12.8 complex, residues 14, 16, 18, and 29 showed large shift perturbations (normalized weighted average shift of >0.5), but Lys29 was less sensitive to cross-saturation than the first three residues. With the Fab 12.10 complex, shift values of >0.5 were observed for residues 5−7, 15, 20, and 83. Three of these residues (6, 7, and 15) displayed a high sensitivity to cross-saturation. Possible explanations for the large shift perturbations without high cross-saturation sensitivity are (1) an effect resulting from antibody contact with the side chain of a given residue, or an adjacent residue, without proximity to the amide group itself and (2) close contact with an antibody group such as a carboxylate that can cause shift perturbation, but lacks protons for saturation transfer.

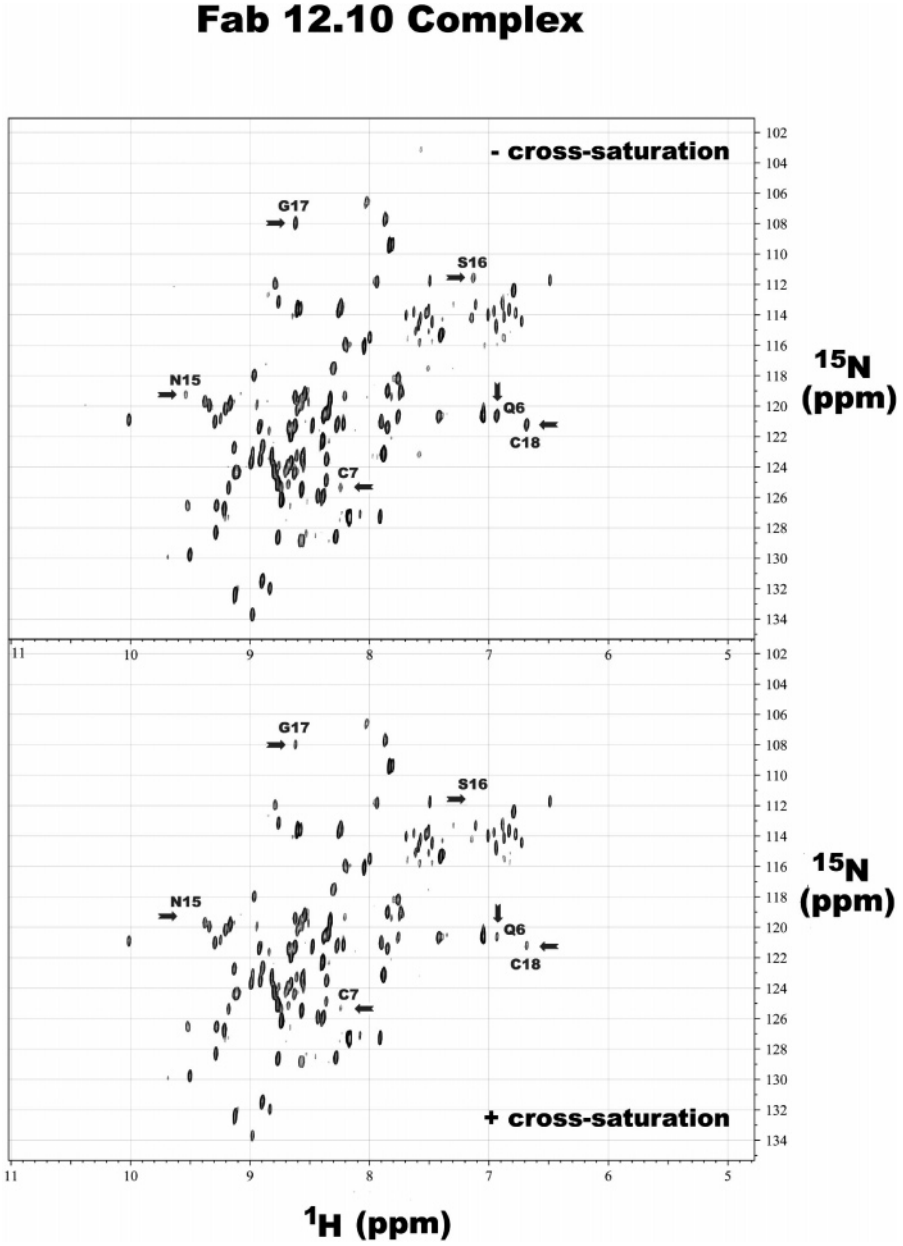

FIGURE 2: TROSY spectra of the Fab 12.10 complex with (bottom panel) and without (top panel) cross-saturation, as in Figure 1.

DISCUSSION

Cross-saturation mapping of the epitopes recognized by these two parasite inhibitory anti- $MSP1_{19}$ monoclonal antibodies exhibited a remarkable degree of similarity. The most affected residues identified for each of the inhibitory monoclonal antibodies cluster in a region located on one of the two broad surfaces of the disk-shaped $MSP1_{19}$ molecule (Figure 4). This surface contains more neutral hydrophilic residues, as well as a few solvent-exposed hydrophobic residues. In contrast, the opposite side of the disk contains more charged residues (both positive and negative) (*9*).

The two inhibitory antibody fragments are both in close contact with backbone amide groups of residues that form the first β-sheet segment of EGF domain 1. In the case of Fab 12.8, this cluster extends for one additional residue (Gln14) around the tight turn that precedes the β-sheet strand. For Fab 12.10, there are additional contacts with a portion of the N-terminal segment (at Gln6 and Cys7), which is directly linked to other contact residues by the Cys7−Cys18 disulfide bridge. This first β-sheet segment faces EGF domain 2, and contains several residues that are involved in interdomain contact. A shallow pocket is formed between the β-sheet strand and the final loop segment of domain 2 (residues 86−92). We speculate that the region of this pocket, which is occluded by binding of these two inhibitory antibodies, may represent a functional site involved in erythrocyte invasion and/or $MSP1_{19}$ processing. This region is well-conserved among human and rodent malaria species (Figure 5).

Interface contacts detected in these experiments have been mapped on the solution structure of the free $MSP1_{19}$ antigen in Figure 4. The question of potential conformational changes in the antigen upon antibody binding should be considered. Several lines of evidence suggest that the extent of conformational change in the antigen is limited in this case. The pattern of slowly exchanging amide groups is unchanged,

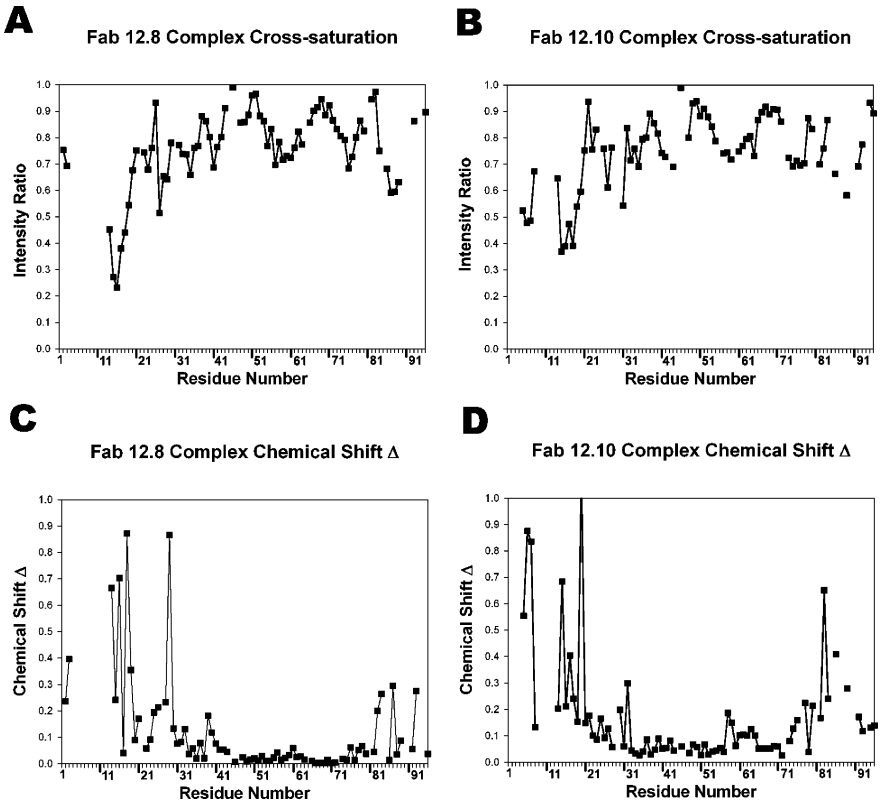

FIGURE 3: Summary of cross-saturation and chemical shift perturbation results for each residue. (A) Cross-saturation for the Fab 12.8 complex. (B) Cross-saturation for the Fab 12.10 complex. (C) Chemical shift perturbation for the Fab 12.8 complex. (D) Chemical shift perturbation for the Fab 12.10 complex. The data shown are for a saturation time of 1.6 s.

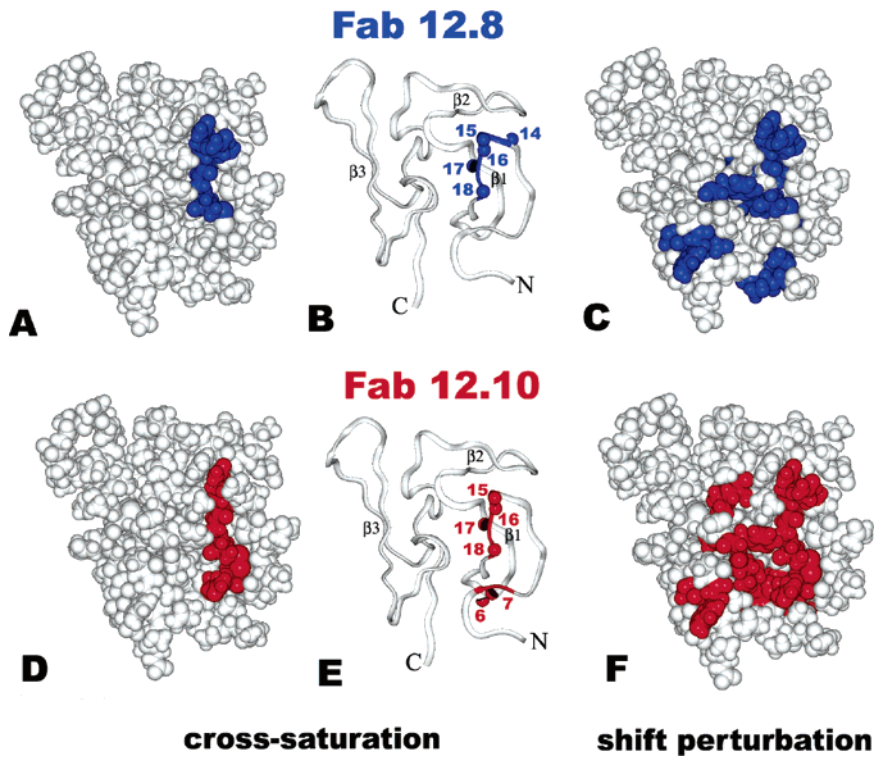

FIGURE 4: Interface residues for the *P. falciparum* $MSP1_{19}$−Fab complexes mapped by TROSY NMR. The residues most sensitive to cross-saturation (less than 50% relative intensity after a saturation time of 1.6 s) are indicated by color (blue for Fab 12.8 and red for Fab 12.10) on the antigen surface (panels A and D). The amide groups of the same residues are also identified on the ribbon diagram (panels B and E). Residues that experienced a large chemical shift perturbation ($\Delta > 0.2$ ppm) are displayed in color in panels C and F. The results are shown mapped onto a representative structure of the free antigen from the NMR ensemble (Protein Data Bank entry 1cej).

indicating that the hydrogen bond network remains intact. This means that the secondary structure β-sheet and tight turn elements are not affected. Furthermore, each EGF-like domain is constrained by three disulfide bridges. The ^{13}C

FIGURE 5: Aligned sequences of selected segments of MSP1$_{19}$ that form the region occluded by binding of the two inhibitory antibodies to *P. falciparum* MSP1$_{19}$. Human and rodent malaria species were aligned with Clustal X. The numbering follows the *P. falciparum* sequence. Within these 18 residues, there are eight invariant positions (red), seven positions in which two forms occur, with conservative amino acid substitutions (orange), and three more variable positions (black). Position 14 in *P. falciparum* is a common dimorphism in different strains, with either Q or E at this site.

shifts of C_α, C_β, and C′ atoms are sensitive to backbone conformation. The ^{13}C chemical shift differences of these signals in the Fab complexes compared to the free antigen are plotted for each residue in Figure 3 of the Supporting Information. There are no continuous stretches of residues with large ^{13}C shift differences that would indicate major backbone conformational changes, as observed, for example, in the study of human ferredoxin (*10*). The above considerations show that mapping interfacial residues on the free antigen structure is valid. The largest ^{13}C shifts (combined C_α, C_β, and C′ shifts of >2.0 ppm) were observed for residues 3, 16, 26, 28, and 31 with the Fab 12.8 complex and for residues 5, 15, 31, and 86 for the Fab 12.10 complex. These effects may be direct shift perturbations by the antibodies, but the possibility of local conformational changes near these residues should also be considered in further structural work and computational modeling.

The TROSY technique, coupled with cross-saturation, represents an excellent approach to mapping conformational epitopes on complete, folded protein antigens. It is important to remember that, while this effectively localizes the epitope, it directly detects the proximity of the antibody only to backbone amide groups in the antigen. However, much of the antibody specificity is presumably derived from side chain−side chain contacts. This problem could be approached by modeling the antibody structure, and investigating protein−protein interactions with theoretical docking calculations. Reliable knowledge of the epitope on the antigen, as obtained here from NMR cross-saturation, will provide invaluable constraints to guide these calculations (*11*). This may prove to be a valuable general approach to the problem of antibody−antigen interactions, as crystallization can be difficult and slow. Precise mapping of the epitopes recognized by these inhibitory monoclonal antibodies has important implications for rational vaccine design and development of antibody-based therapeutics. In the case of a specific anti-HIV gp120 monoclonal antibody, efforts to selectively produce an immune response with similar specificity have been termed "immunofocusing" (*12*). A similar approach may also be possible with MSP1$_{19}$. Furthermore, with *P. falciparum* MSP1$_{19}$, the phenomenon of "blocking" antibodies has been described. These are antibodies that compete with inhibitory antibodies 12.8 and 12.10 and thus interfere with their antiparasite activity, while possessing no inhibitory activity themselves. Amino acid substitutions in the MSP1$_{19}$ antigen that prevent binding of blocking but not of inhibitory antibodies have been studied (*1*). More precise knowledge of the location of inhibitory epitopes will help guide further efforts with these rational vaccine design approaches.

SUPPORTING INFORMATION AVAILABLE

Sample time courses of cross-saturation experiments (Figure 1), time courses for residues with high cross-saturation sensitivity (Figure 2), backbone ^{13}C chemical shift differences in Fab complexes (Figure 3), and resonance assignments for free MSP1$_{19}$ and Fab complexes (Table 1). This material is available free of charge via the Internet at http://pubs.acs.org.

REFERENCES

1. Uthaipibull, C., Aufiero, B., Syed, S. E. H., Hansen, B., Guevara Patiño, J. A., Angov, E., Ling, I. T., Fegeding, K., Morgan, W. D., Ockenhouse, C., Birdsall, B., Feeney, J., Lyon, J. A., and Holder, A. A. (2001) Inhibitory and blocking monoclonal antibody epitopes on merozoite surface protein 1 of the malaria parasite *Plasmodium falciparum*, *J. Mol. Biol. 307*, 1381−1394.
2. Dekker, C., Uthaipibull, C., Calder, L. J., Lock, M., Grainger, M., Morgan, W. D., Dodson, G. G., and Holder, A. A. (2004) Inhibitory and neutral antibodies to *Plasmodium falciparum* MSP1$_{19}$ form ring structures with their antigen, *Mol. Biochem. Parasitol. 137*, 143−149.
3. Morgan, W. D., Lock, M. J., Frenkiel, T. A., Grainger, M., and Holder, A. A. (2004) Malaria Parasite-Inhibitory Antibody Epitopes on *Plasmodium falciparum* Merozoite Surface Protein-1$_{19}$ Mapped by TROSY NMR, *Mol. Biochem. Parasitol. 138*, 29−36.
4. Pervushin, K., Riek, R., Wider, G., and Wuethrich, K. (1997) Attenuated T2 relaxation by mutual cancellation of dipole−dipole coupling and chemical shift anisotropy indicates an avenue to NMR structures of very large biological macromolecules in solution, *Proc. Natl. Acad. Sci. U.S.A. 94*, 12366−12371.
5. Pervushin, K., Wider, G., and Wuethrich, K. (1998) Single transition-to-single transition polarization transfer (ST2-PT) in [^{15}N,^{1}H]-TROSY, *J. Biomol. NMR 12*, 345−348.
6. Takahashi, H., Nakanishi, T., Kami, K., Arata, Y., and Shimada, I. (2000) A novel NMR method for determining the interface of large protein−protein complexes, *Nat. Struct. Biol. 7*, 220−223.
7. Delaglio, F., Grzesiek, S., Vuister, G. W., Zhu, G., Pfeifer, J., and Bax, A. (1995) NMRPipe: A multidimensional spectral processing system based on UNIX pipes, *J. Biomol. NMR 6*, 277−293.
8. Yang, D., and Kay, L. E. (1999) TROSY Triple-Resonance Four-Dimensional NMR Spectroscopy of a 46 ns Tumbling Protein, *J. Am. Chem. Soc. 121*, 2571−2575.
9. Morgan, W. D., Birdsall, B., Frenkiel, T. A., Gradwell, M. G., Burghaus, P. A., Syed, S. E. H., Uthaipibull, C., Holder, A. A., and Feeney, J. (1999) Solution structure of an EGF module pair from the *Plasmodium falciparum* merozoite surface protein 1, *J. Mol. Biol. 289*, 113−122.
10. Xia, B., Volkman, B. F., and Markley, J. L. (1998) Evidence for Oxidation-State-Dependent Conformational Changes in Human Ferredoxin from Multinuclear, Multidimensional NMR Spectroscopy, *Biochemistry 37*, 3965−3973.
11. Wodak, S. J., and Mendez, R. (2004) Prediction of protein−protein interactions: The CAPRI experiment, its evaluation and implications, *Curr. Opin. Struct. Biol. 14*, 242−249.
12. Pantophlet, R., and Burton, D. R. (2003) Immunofocusing: Antigen engineering to promote the induction of HIV-neutralizing antibodies, *Trends Mol. Med. 9*, 468−473.

BI0482957